Journal of Advances in Science and Technology
Vol. 17, Issue No. 1, March-2020, ISSN 2230-9659

A Study on Humidity Response in DMV-CS Self Assembled Nanofibers

Anil Kumar[1]*, Dr. Sachin Saxena[2]

[1] Research Scholar, Shri Krishna University, Chhatarpur M.P.

[2] Professor, Shri Krishna University, Chhatarpur M.P.

Abstract - The Scope of Research into Low-Dimensional Nanomaterials and Their Potential Technological Applications, Developing superior organic nanostructures calls for a bottom-up strategy, and techniques like self-assembly and layer-by-layer deposition is well adapted to this end. Dodecyl methyl viologen (DMV) and coronene tetracarboxylate (CS) self-assembled nanofibers exhibit remarkable electrical characteristics and have potential applications in devices such as Field Effect Transistors and Humidity Sensors. DMV-CS nanofibers change shape as the surrounding humidity does, as well as what goes into their formation during the drying process. Micelles, which make up DMV-CS SAN, were shown to have an internal hexagonal ordering and elliptical distortion in the individual micelle as humidity was increased.

Keywords - Dodecyl methyl viologen (DMV), coronene tetracarboxylate (CS), Nanofibers

----------X----------

INTRODUCTION

When it comes to developing structural complexity from a constrained set of starting ingredients, self-organization mechanisms in supramolecular materials are strikingly comparable to their biological counterparts. (1) It is challenging, but necessary, to understand how these materials self-assemble in the presence of other species in order to develop new functional devices. Recently, supramolecular design methodologies have become increasingly popular as a means of creating organic materials with novel properties. Supramolecular materials, a relatively new class of organic substances, hold significant promise as possible building blocks for a broad variety of technological applications. (2) The size regime between single molecules (few nm) and polymer thin films (m) is beneficial for the interactions in these materials since it enables simple fabrication. In this context, donor acceptor (D-A) molecules are important because the charge transfer interactions may be modified by changing the kind of organisation due to external factors, leading to different morphologies like 1D nanostructures. D-A couples include, among others, the spherical micellar structure-forming agent's dodecyl methyl viologen (DMV), potassium salt of coronene tetracarboxylate, and pyridine (CS). A micelle of amphiphilic bilayers, with a diameter of about 6 nm and two charge transfer moieties aligned head to tail, is formed when DMV-CS molecules assemble face to face in a solution. Perhaps as a result of their surface charge, micelles can coalesce into nanofibers with a diameter of 50-150 nm and also thicker fibres. With water present, an integrative self-assembly process occurs when both the hydrophilic head and the hydrophobic tail interact. (5) It has been shown that the characteristics of DMV-CS self-assembled nanofibers are profoundly influenced by the relative humidity (RH). The electrical characteristics of nanofibers have been investigated, and it has been proven that, when utilised as the active material in FET devices, they achieve considerable levels of charge carrier mobility. The quick response of the nanofiber-conductivity to even small changes in RH suggests that these fibres may be exploited to develop an ultrafast RH sensor (6, 7). UV-Vis, XRD, and AFM measurements all show that when relative humidity (RH) increases, the d gap corresponding to the - bond of DMV-CS moieties decreases, causing a significant change in conductivity. Whereas ultrafast RH sensors based on a similar supramolecular system have been published, the nanoscopic structural changes in the self-assembled structure of these molecules as a function of dryness have not yet been completely studied. We provide the first evidence that drying the dispersion and exposing the resulting nanofibers to varying equilibrium RH levels modifies the self-assembled internal structure of DMV-CS nanofibers. (8)

HUMIDITY RESPONSE IN DMV-CS

Grazing incidence small angle x-ray scattering (GISAXS) was used to monitor the self-organization of the interior structure of these systems. However, the films used in this work contained nanofibers of such a broad range in diameter that it was unable to collect well-defined Yoneda peaks in the observed GISAXS data. It was also shown that diffuse scattering measurements are affected by the size of

the X-ray beam's footprint (10). Because of this, we analysed Bragg peaks using the born approximation and the effective surface assumptions discussed above. Our in-situ GISAXS experiments with drying of dispersion showed significantly more uneven films than those with spin-coating. In the first set of experiments, relative humidity (RH) was varied in a controlled environment from 5% to 96% while nanofiber films were monitored using GISAXS. In the second set, we utilised x-ray microscopy to watch nanofibers self-assemble on a substrate during drying, taking special care to confine the beam's footprint within the films' shielded regions as the water was removed. (12)

OBJECTIVES OF THE STUDY

- To study the Humidity Response in DMV-CS Self Assembled Nanofibers

RESEARCH METHODOLOGY

Synthesis of CS-DMV nanofibers: Both the CS (donor) and DMV (acceptor) molecules' full synthesis protocols are already public knowledge. We were able to self-assemble CS-DMV into water by dissolving the salts in Millipore water, sonicating the solution for 5 minutes, and then mixing equal volumes of the DMV and CS solutions. This water was then utilised to create charge transfer (CT) nanofibers. To create a hierarchical self-assembly, we use ground-state CT interactions between D and A pairs of the potassium salt of coronene tetracarboxylate (CS) and the dodecyl substituted unsymmetrical viologen derivative (DMV). The RH-dependent switching tests conducted on films made from solutions of varied concentrations led to the conclusion that 2mM was the best solvent concentration for this set of experiments.

Grazing Incidence Small Angle X-Ray Scattering

Here we provide GISAXS data collected from KEK's Photon Factory's Indian Beamline in Japan. The sample was kept on a silicon substrate and illuminated at a distance of 3902 mm using a monochromatic X-ray source with a wavelength of 10.138 keV. The beam used had a height of 0.3mm, a width of 1mm, and an incidence angle of 0.4o. Pixels on the PILATUS-1M detector were 172 m on a side.

Experiments with drying a drop of 2mM solution (approximately 10 L) were performed on a pre-aligned substrate covering an area of less than one centimetre squared, and the beam's imprint was retained deep below the formed-film of cylindrical micelles. The drying time of an aqueous dispersion in the air at 30% relative humidity was measured over the course of 20 minutes, and this time period is represented by a series of 30-second time snapshots. An aluminium cell with kapton windows was used to allow the incident and scattered X-rays to pass through to the sample in the middle. The free volume of the container was used to store a number of different saturated salt solutions, each of which had a slightly different equilibrium vapour pressure. The DTH11 RH censor connected to an Arudiano Uno served as both a metre and a calibrator within the cell. To get the humidity down to 5% RH, a sealed dry cell was used to continuously pump in dry Helium gas. In a hutch with an ambient RH of 30%, we were able to achieve RH values of 52%, 75%, 85%, and 96% by adding saturated salt solutions of Mg(NO3)2, NaCl, KCl, and K2SO4. WAKO Chemicals Japan supplied all of the ultra-pure chemicals. GISAXS data was collected when the RH value remained below 1% after the solution was added and the cell was allowed to equilibrate for 15 minutes.

RESULTS

Aridity dependent distortion of nanofibers

X-ray transmission was achieved by placing the sample on a silicon substrate within a cylindrical cell with Kapton windows. Since the grazing angle of incidence was set to 0.4o, the in-plane components of the wave-vectors, namely qy and qx, remained zero at scattering angle 2, providing a finite value of qz =(4/)Sin. The three components of the wave vector q are all non-zero in all other detector pixels (qx, qy, and qz). In this geometry, the values of qz and qy differ substantially along the vertical and horizontal axes. Quantitative analysis may be performed using 1D intensity profiles created by data reduction techniques, Qz cuts, or 1D data in the qz direction, were created by integrating a small number of pixels at qy=0. Another piece of information that was extracted from the 2D data was the angular cut, which plots the intensity distribution against the scattering angle. In order to examine lower-intensity peaks, we created qy cuts towards the top, at 60 degrees. The near hexagonal symmetry of the nanofibers is seen in the raw 2D data as a function of RH. For example, peaks in the diffraction pattern's qz and qy directions may be labelled as (0, 0, 2) and (0, -1, 1).

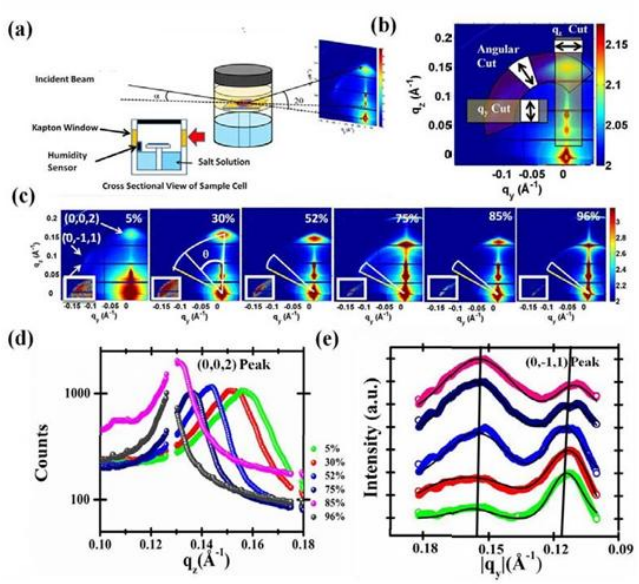

Anil Kumar[1]*, Dr. Sachin Saxena[2]

Figure 1: (a) sample cell and experimental setup used to quantify DMV-CS fibres using RH-dependent GISAXS. (b) The 2D GISAXS data collected by the PILATUS 1M detector is given with a variety of techniques for its transformation into 1D slice. There is a black arrow in each white box cell, pointing in the direction of pixel integration. (c) DMV-CS nanofiber on Si substrate GISAXS data as a function of relative humidity. According to the lattice model shown in Figure 4.3, the angular separation between the two diffraction spots seen is (0, 0, -1) and (0, -1, 1). (d) Are marked off - the location of a hexagonal lattice that's absolutely flawless

The spot's location (yellow line) and the position of the observing device (white line) are both displayed. The distortion clearly gets better as the RH levels get up. The RH-dependent intensity profiles in the qz and qy directions are illustrated graphically in panels (d) and (e) of the 2D detector data. The (0, 0, 2) peak is seen in the qz data, while the lamellar structure and the (0, -1, 1) reflection are seen in the qy data.

When humidity is raised from 5% to 96%, the average fibre width increases from 5.7 nm to 5.96 nm, and the unit cell volume per unit fibre length climbs from 45.7 nm3 to 60.4 nm3. Assuming that the volume change is due only to the addition of water molecules, the expected number of extra water molecules per nanometer length of these fibres turns out to be 490. Interaction with these extra water molecules accounts for the shorter - bond length previously shown.

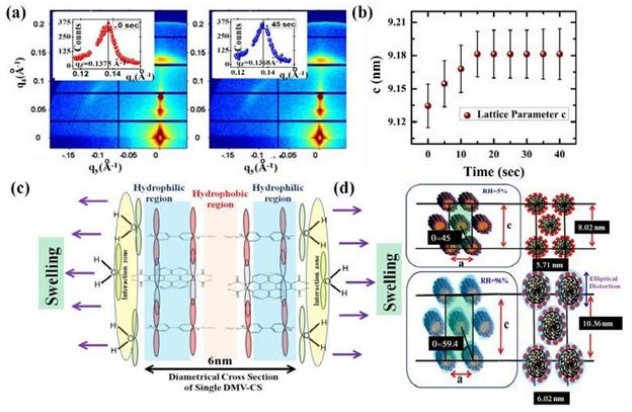

Figure 2: (a) GISAXS pictures of DMV-CS film during transition from RH 52% (left) to RH 75% (right) with insets showing the (0, 0, 2) peak along qz direction. The fast change in the lattice parameter 'c' with time is illustrated in the extreme right panel with error bars as the RH value is adjusted from 52% to 75% - equilibrium condition is obtained in roughly 20 Sec. (c) Two DMV-CS molecules are stacked back-to-back along the diameter of a standard micelle in this schematic representation of a nanofiber's cross section. Inside the micelle, where the hydrophobic hydrocarbon chains of DMV molecules are aligned with one other, is the hydrophobic zone. The DMV-CS charge transfer complex has a hydrophilic zone, which is the outermost layer of the cylinder. (d) Using a Face Centered lattice with in-plane and out-of-plane lattice parameters a and c, the atomic structure and structural exfoliation of DMV-CS were studied. It is a complete hexagonal lattice with a reflection angle of 60 degrees between the (0, 0, 2) and (0, -1, 1) planes for c=3a.

It is possible to deduce each micelle's shape transformation intuitively using the Curie principle of scattering, which asserts that the symmetry of the diffraction spot seen must be the same as the symmetry of the scatterer. How the diffraction spot is shaped depends on the form factor of each micelle. The spot's form changes from circular to elliptical when relative humidity (RH) rises, as seen by the intensity contour of the (0, 0, 2) peak. The ellipse's principal axis runs in the qy plane. As the relative humidity (RH) of the surrounding air rises, the typical fiber's cross section changes shape from circular to elliptical, with the major axis pointing out of the plane of the fibre. Extracting the intensity profile of the (0, 0, 2) peak along the qz and qy directions allowed us to calculate the intensity-shape I(qy, qz) of the (0, 0, 2) peak, which allowed us to quantify the elliptical distortion. An elliptical symmetry in the diffraction spots appears due to an elliptical shape shift at the higher RH values, but the better hexagonal symmetry is gained in this case. It was found that the successful transition from a circular to an elliptical shape might be undone.

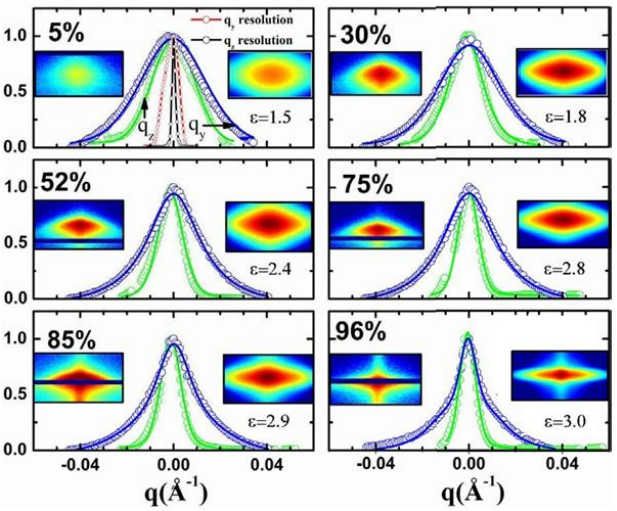

Figure 3: Humidity in the qz (green) and qy (blue) directions throughout the (0, 0, 2) location, depicted on the same scale as the intensity profile

Self Assembly of nanofibers during drying

By keeping the X-ray beam focused on a drop of 2mM DMV- CS solution on a hydrophobic silicon substrate and continually collecting data as the solution evaporated, GISAXS measurements could

be carried out in real time. Over time, DMV-CS nanofibers underwent a structural transformation on the inside. Data was captured every 30 seconds using the PILATUS 1M detector to provide real-time insight into the drying process. For instance, DMV-CS micelle may be freely moving with other unassembled or partially assembled conglomerates in the organic matrix after just 300 seconds of drying, showing the absence of any organised structure. The only telltale signs of a Kapton window, the specular spot and powder ring, are absent from this image. The micelle concentration increases as the drop's water evaporates, and the micelles' hydrophilic surfaces start to combine. After 330 s, the initial ordering of the DMV-CS molecules is reflected in the GISAXS data as a single isolated spot (see the second frame of Figure 4.5(a)) at qz=1.4 nm-1, indicating the existence of a layered lamellar structure. In order to lessen the repulsion between the hydrophilic heads and the hydrophobic tails, a lamellar stack forms parallel to the hydrophilic substrate, as shown by the patch along the qz axis. After 420s (from the fourth frame forward), the micelles settle into a hexagonal lattice form as the solvent content decreases. Spot placements that move further apart in q space, indicating a reduction in the lattice parameters (refer to qz cuts around the (0, 0, 2) peak, may be used to trace the shifting order of the DMV-CS molecules as they dry. When the 750 seconds are up, the film is completely dry, and the average fibre diameter, as determined by the lattice parameter a, has shrunk from 5.77 nm to 5.41 nm. We were able to see the growth of the first lamellar peak by slicing the GISAXS data recorded as a function of drying time into qy planes. Even in 270s data, we see a sizable peak at qy=1.4nm-1, indicating that the lamellar stacks in DMV-CS are not all lying in a plane perpendicular to the substrate. In the presence of increasing qy, this peak moves upwards until it reaches its final value of 1.54 nm-1. Seeing the lamellar peak shift in qz cuts was difficult due to the presence of a strong (0, 0, 2) peak. Since the peak-position shifts when the evaporation time goes from 270 to 390 seconds, this shows that the lamellar phase becomes more compact and the lamellar stacking shifts from 4.43 to 4.1 nm. After 400 seconds of drying, a hexagonal peak with coordinates (0, -1, -1) has formed. It should be stressed that the observation of a single peak in both types of investigations is the basis for this proposed presence of a lamellar phase. Detailed structural analysis is required to make sense of this phase.

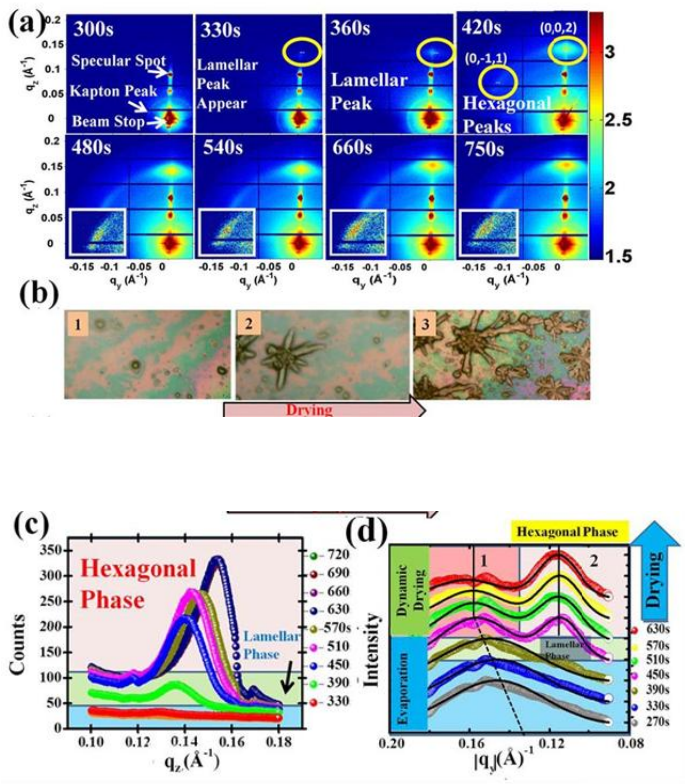

Figure 4: Changes in DMV-CS nanofiber concentration and size distribution as a function of drying time

When the concentration of DMV and CS molecules increases due to water evaporation, the optical micrographs reveal the expansion of the nucleation centre and the formation of long tubes in the dendrimeric structure resembling a star. As GISAXS data from a drying experiment demonstrates, a lamellar structure with a periodicity of around 4 nm forms first, followed by long fibres with a hexagonal cross section. Lamellar peaks are most evident in the qz direction, but may be seen in qy scans as well, indicating that the lamellar phase prefers to be oriented parallel to the hydrophilic substrate. A greater DMV-CS concentration results in a more compact lamellar structure and a higher q value of 1.54 nm-1 when the solution evaporates. This lamellar peak at this q value was also seen in the experiment when humidity was strictly controlled.

In this case, the nanofibers' propensity for a hexagonal packing configuration and the correlation between relative humidity (RH) and drying time (T). With the equilibrium RH value and tDD (=750 - drying time in seconds) along the x-axis and zero indicating the conclusion of the drying process, we can directly compare the essential characteristics of the deformed hexagonal lattice in Figure 4.6. Keep in mind that the ambient RH in the experimental hutch was 30%; as a result, the obtained values of the drying experiment parameters did not change until they reached the ambient RH value.

Results from in-situ GISAXS measurements done to learn more about the self-organization of DMV-CS nanofibers in response to moisture content. It was shown that an increase in relative humidity causes the hexagonal lattice of the DMV-CS micelle to expand and become less distorted. The results of the drying experiment demonstrated the multistage nature of self-assembly processes. As the DMV-CS concentration inside the droplet rises, the GISAXS data unambiguously show the presence of the lamellar phase in the first stage. Further ageing has resulted in the lamellar stacking's transformation into distorted hexagonal cylinders of nanofibers. We have run model simulations to quantify the observed elliptical shape distortion of the attached nanofibers, which occurs because the nanofibers are not secured to the substrate during the manufacturing step. The structural deformation of the deformed hexagonal lattice and the elliptical distortion in the individual nanofiber were found to be significantly affected by the ambient RH value. Because of this discovery, we now know why nanofibers react so rapidly to changes in humidity.

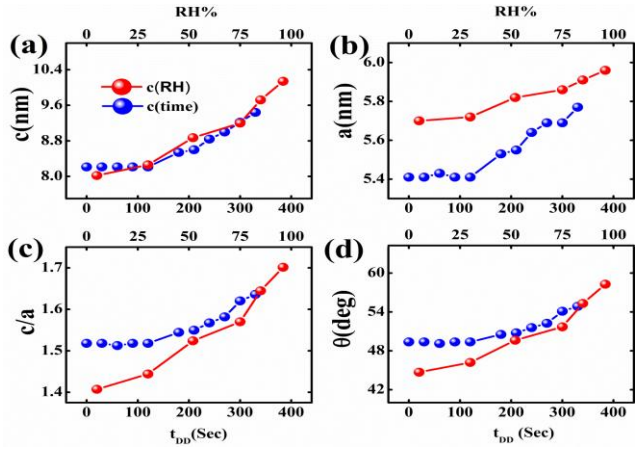

Figure 5: Results from drying tests were compared to those from humidity trials, with tDD set as 750 seconds.

Transport Measurement of DMV-CS Nanofiber

Drops of the CS-DMV nanofibre solution (5 L, 1 mM) were drop coated onto gold gap electrodes on glass and allowed to dry for one hour before transport measurements were taken. The item was placed in a humidity cell, and its electrical properties were characterised using a Keithley 4200 source unit. The humidity cell was filled with a mixture of air, nitrogen, and water vapour of varying relative humidities.

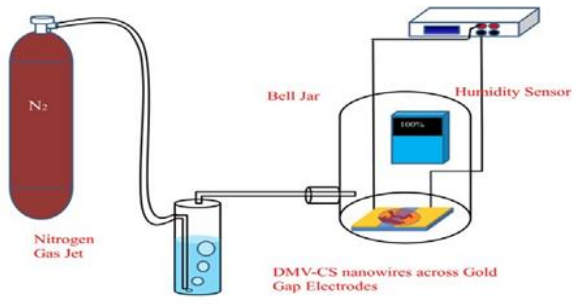

Figure 6: Humidity dependent transport measurement apparatus of DMV-CS Hydrogels

In this experiment, we observe the humidity-dependent characterizations of a 2mM DMV-CS hydrogel, which causes the hydrogel to switch behaviour. The effectiveness of 2mM DMV-CS hydrogel is significantly impacted by ambient humidity. Humidity and water molecules more generally, play a significant part in the conduction process governed by DMV-CS molecules, as seen by the considerable decrease in resistance seen as humidity increases. Exposure to higher degrees of humidity has been demonstrated to directly alter nanofiber transport capabilities, however the exact mechanism is still being researched. As we observed in the preceding section, the humidity quickly alters the lattice structure of the nanofibers and the shape of the individual micelle. Wax-absorption X-ray spectroscopy (WAXS) studies of the nanowires showed that the same deformation caused a general shortening of the bond length of DMV-CS self-assembled nanofibers when the relative humidity of the air varied. The lattice distortion brought on by the water molecules is thought to be the root cause of the electrical channel within the fibres shrinking, leading to decreased resistance at higher humidity levels. Unfortunately, researchers have yet to determine the system's specific transport mechanism.

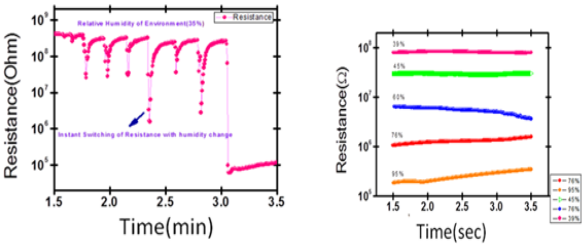

Figure 7: (a) Humidity dependent Switching of DMV-CS Hydrogels. (b) Humidity dependent resistance of theDMV-CS Hydrogels

CONCLUSION

Grazing Incidence Small Angle X-Ray Diffraction analysis of a drop-cast sample on a substrate showed that the DMV-CS self-assembled nanofibers exhibit an internal symmetry of hexagonal ordering. Humidity-dependent analyses of DMV-CS nanofibers also indicated that they had a high affinity for water molecules, which causes them to expand when the water is absorbed into the micelle's lattice. Spot shape study of DMV-CS nanofibers revealed elliptical micelle distortion in the out-of-plane direction, whereas the overall micelle lattice evolved from a distorted hexagonal to aless distorted hexagonal with increasing humidity.

REFERENCES

1. Mogera, U., Sagade, A. A., George, S. J. & Kulkarni, G. U. Ultrafast response humidity sensor using supramolecular nanofibre and its application in monitoring breath humidity and flow. Sci. Rep. 4, 4103 (2014).
2. Li, Y., Liu, T., Liu, H., Tian, M.-Z. & Li, Y. Self-assembly of intramolecular charge-transfer compounds into functional molecular systems. Acc. Chem. Res. 47, 1186–98 (2014).
3. Sagade, A. A. et al. High-mobility field effect transistors based on supramolecular charge transfer nanofibres. Adv. Mater. 25, 559–64 (2013).
4. Operamolla, A. & Farinola, G. M. Molecular and Supramolecular Architectures of Organic Semiconductors for Field-Effect Transistor Devices and Sensors: A Synthetic Chemical Perspective. European J. Org. Chem. 2011, 423–450 (2011).
5. Rao, K. V., Jayaramulu, K., Maji, T. K. & George, S. J. Supramolecular hydrogels and highaspect-ratio nanofibers through charge-transfer-induced alternate coassembly. Angew. Chemie - Int. Ed. 49, 4218–4222 (2010).
6. Wang, C. et al. Controlled Self-Assembly Manipulated by Charge-Transfer Interactions: From Tubes to Vesicles. Angew. Chemie 120, 9189–9192 (2008).
7. Vuillaume, D. et al. Electronic properties of organic monolayers and molecular devices. Pramana 67, 17–32 (2006).
8. Pal, S., Sanyal, M. K., John, N. S. & Kulkarni, G. U. Formation of a rectifier with gold nanoclusters: X-ray reflectivity and atomic force microscopy measurements. Phys. Rev. B 71, 121404 (2005).
9. Fichtner, M. Cover Picture: Nanotechnological Aspects in Materials for Hydrogen Storage (Adv. Eng. Mater. 6/2005). Adv. Eng. Mater. 7, NA-NA (2005).
10. Matsui, I. Nanoparticles for Electronic Device Applications: A Brief Review. J. Chem. Eng. JAPAN 38, 535–546 (2005).
11. Alivisatos, P. The use of nanocrystals in biological detection. Nat. Biotechnol. 22, 47–52 (2004).
12. Bueno, J. T., Shchukina, N. & Ramos, A. A. A substantial amount of hidden magnetic energy in the quiet Sun. Nature 430, 326–329 (2004).

Corresponding Author

Anil Kumar*

Research Scholar, Shri Krishna University, Chhatarpur M.P.